Comparative study of detection of COVID-19 using Transfer Learning

Shikhar Vaish, Student, Bharati Vidyapeeth (Deemed to be University) College of Engineering, Pune, shikhar.vaish-coep@bvucoep.edu.in

Preksha Jagetiya, Student, Bharati Vidyapeeth (Deemed to be University) College of Engineering, Pune, preksha.jagetiya-coep@bvucoep.edu.in

Gauri Sharma, Student, Bharati Vidyapeeth (Deemed to be University) College of Engineering, Pune, gauri.sharma-coep@bvucoep.edu.in

Gajanan Bhole, Assistant Professor, Bharati Vidyapeeth (Deemed to be University) College of Engineering, Pune, gvbhole@bvucoep.edu.in

Abstract: Early identification, isolation and care for patients is a key strategy for better management of this pandemic. Our study will aim to provide a theoretical transfer learning framework to support COVID-19 detection with the use of image classification using deep learning models for multiple imaging modes including X-Ray and CT scan. This study will focus on X-Ray and CT-Scan images only and provide timely model selection guidelines to the practitioners who often are resorted to utilising a certain mode of imaging due to time and resource scarcity. This could also assist practitioners and researchers in developing a supporting tool for highly constrained health professionals in determining the course of treatment depending on severity. Initial testing will also be conducted to understand the suitability of various popular pre-trained models for transfer learning like Xception, VGG19, Inception, Resnet etc. In the end, we will be comparing the accuracies of both X-Ray and CT-Scan to determine which technique gives more accurate results.

Keywords —Convolutional neural networks (CNNs), COVID-19, transfer learning, X-Ray, Deep Learning, CT-Scan

I. INTRODUCTION

Coronaviruses are a very huge family of different viruses constituting the subfamily Orthocoronavirinae. Some of them are responsible for causing the common cold in people. Others infect animals, including bats, camels, and cattle. But how did the new coronavirus that causes COVID-19, come into being?

Novel coronavirus-causing Covid-19 disease has been formally named as Severe Acute Respiratory Syndrome Coronavirus-2 (SARS-COV-2) [1].

Experts say SARS-CoV-2 originated in bats. That is the same way how the coronaviruses behind the Middle East respiratory syndrome (MERS) and severe acute respiratory syndrome (SARS) got started. SARS-CoV-2 (Covid-19) transmitted to humans at one of Wuhan's "wet markets". This place is one of the most populous cities and famous for customers buying fresh meat and fish, including animals that are killed on the spot. Some wet markets also sell wild or banned species of animals like cobras, wild boars, and raccoon dogs. Overcrowded conditions can let viruses from different animals swap genes. Sometimes the virus's genetic information changes so much that it can transmit and infect people [2].

As SARS-CoV-2 started to spread, it infected people who have had no direct contact with animals. This growing worldwide transmission is what is now a pandemic as declared by WHO in March 2020[2]. The current COVID-19 pandemic has impacted the world with over 169 million infections and over 3.5 million deaths so far(as of 29 May 2021) [3].

Few symptoms of COVID-19 are dry cough, fever, tiredness, respiratory diseases which lead to pneumonia in some cases, chest pain etc [4]. In about 74% of the cases, the COVID-19 causes mild (18%) or moderate (56%) symptoms. However, the remainder of the cases range from critical (20%) to severe (6%) [5].

Generally, pneumonia is an infection that causes inflammation to air sacs present in the lungs for oxygen transfer. The other types of pneumonia infection include fungi, bacteria, and other viruses causing disease.

The reason for severity is chronic diseases such as bronchitis or asthma, diabetes, hypertension, heart diseases etc. The infected people are treated based on the infected organism, however, pain reliever, fever reducer, cough medicine and

 DOI : 10.35291/2454-9150.2021.0270

antibiotics are given to patients based on symptoms. If the patient is grievously affected by infection, they have to be hospitalized in the Intensive Care Unit (ICU) and treated suitably. If breathing is difficult, ventilators are to be provided for the same [6]. The COVID-19 is declared a pandemic due to its seriousness and faster transmissibility rate [7].

The impact is greater in the healthcare department due to the number of people getting affected day by day. There will be more demand for mechanical ventilators for a serious patient admitted to ICU. Hence, the number of beds in ICU also needs to be increased significantly [8]. In the above situation, the initial diagnosis is crucial for proper treatment which, in turn, reduces the pressure on the health care system.

Fast, affordable, accessible and reliable identification of COVID-19 pathology in an individual is key to slowing the transmission of COVID-19 infection. Reverse transcriptase quantitative polymerase chain reaction (RT-qPCR) tests are the gold standard for diagnosing COVID-19 [9]. During this test, small amounts of viral RNA are extracted from a nasal swab, amplified, and quantised with virus detection indicated visually using a fluorescent dye. Unfortunately, the RT-qPCR test is manual and time-consuming, with results taking up to two days. Some studies have also shown false positive Polymerase Chain Reaction PCR testing [10].

Other testing techniques include imaging technology-based approaches using Computed Tomography (CT) imaging [11], X-Ray imaging-based [12], [13] and Ultrasound imaging [14].

Virus tests take less time as new technologies are developing worldwide. The diagnosis of COVID-19 infection involves a chest scan to verify the condition of the lungs, in such a way that, if the patient shows pneumonia in the scans, they are considered to have a COVID-19 infection. This method allows authorities to isolate and treat affected patients in a timely and affirmative fashion [15].

On 30 June 2020, Dr KK Aggarwal, President of Heart Care Foundation of India told in one of his videos on YouTube if any Covid-19 suspected or confirmed case comes up and he has only the Chest X-Ray of the patient available, he uses pneumonia patches number in X-Ray to decide whether patient needs to hospitalised and require ventilator or not.

If there are two patches in the X-Ray, the patient needs to be hospitalised. Whereas if there are three pneumonia patches, the patient is kept on a ventilator [16].

The diagnostic tools for COVID-19 from multiple imaging modes such as X-Ray, Computerized Tomography (CT Scan), and Ultrasound would provide an automated second

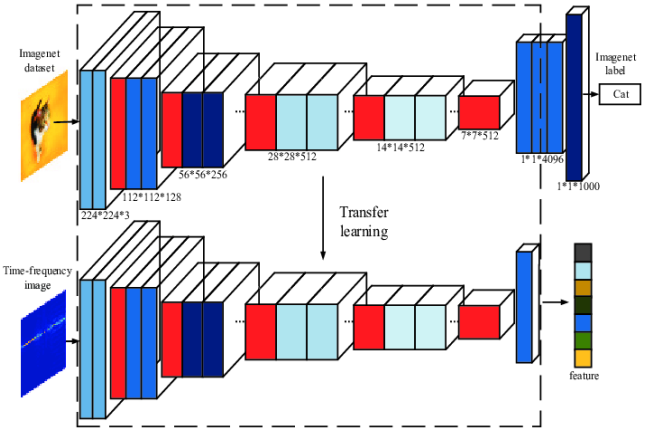

FIG 1: Shows Feature Extraction by Transfer Learning Technique[25]

reading" to doctors, assisting in the diagnosis and criticality assessment of COVID-19 patients to assist in better decision making in the global fight against the disease. COVID-19 often results in pneumonia, and for radiologists and practitioners differentiating between COVID-19 pneumonia and other types of pneumonia (viral and bacterial) solely based on diagnostic images could be challenging [17]. Deep learning artificial neural networks, and the Convolutional Neural Networks (CNNs) have proven to be highly effective in a vast range of medical image classification applications [18], [19]. The accession of a sufficiently large and publicly available collection of medical images data samples for fully training the deep learning models is challenging for the novel nature of COVID-19 since gathering and labelling of images requires significant time and resources to compile. An alternative method of training deep learning models is transfer learning in which a deep learning network is pre-weighted with the results of a previous training cycle from a different domain [20], [21].

Transfer learning is a technique that makes use of the knowledge attained by a CNN from a pre-defined problem to solve a distinct but similar task. This transferred knowledge is used in a new dataset, whose size is usually smaller than the adequate size to train a CNN from scratch [22]. In deep learning, this method requires initial training using large datasets for a given task. The availability of a considerable size dataset is the main factor in ensuring the technique's success since CNN can learn to extract the most significant features of a sample. The CNN is deemed suitable for transfer learning if found to extract the most important image features [23].

Then, in transfer learning, the CNN is used to analyse a new dataset of a different nature and extract its features according to the information acquired in the first training. One common strategy to exploit the capabilities of the pre-trained CNN is called feature extraction via transfer learning [24]. This approach is used so that the CNN will retain its architecture and weights between its layers; therefore, used only as a feature extractor. The features are later used in a second classifier/network that will process its classification. In FIG 1 we can see how feature extraction takes place through

 DOI : 10.35291/2454-9150.2021.0270

transfer learning [25].

II. CLASSIFICATION OF MODELS:

i. RESNET

A ResNet, short for Residual Networks, is a classic artificial neural network (ANN) of a kind that builds on constructs known from pyramidal cells in the cerebral cortex [26].

Residual Block: The problem of training very deep networks introduced ResNet. ResNets are made up of Residual Blocks. The residual network concept was introduced by this architecture to solve the problem of the vanishing/exploding gradient. A technique called skip connections was used for deep architectures that skip some layer in the neural network and connect directly to the output [27].

The core idea of ResNet is introducing "identity shortcut connection" [28]. It skips one or more layers and uses that to deal with vanishing gradient issues. Stacking layers would not degrade the network performance, simply because we could stack identity mappings upon the current network, and the resulting architecture would perform the same.

ii. VGGNet:

VGGNet performed very well in the ImageNet Large Scale Visual Recognition Challenge in 2014. VGG was a breakthrough in Convolutional Neural Networks[29]. It is an innovative object-recognition model that supports up to 19 layers. VGG incorporates 1x1 convolutional layers to make the decision function more nonlinear without changing the receptive fields. The small-size convolution filters allow VGG to have a large number of weight layers and more layers lead to improved performance.

The VGG16 and VGG19 are convolutional neural network architectures with very small convolution filters (3 × 3) and a stride of 1 designed to achieve high accuracy in large-scale image recognition applications[30].

The VGG16 is a convolutional neural network model. It was proposed by A. Zisserman and K. Simonyan in the paper "Very Deep Convolutional Networks for Large-Scale Image Recognition". It was also used to win the ILSVRC competition in 2014[31]. You can load a pre-trained version of the network trained on more than a million images from the ImageNet database and can classify images into 1000 object categories, such as keyboard, mouse, pencil, and many animals.

The VGG-19 network is trained on more than one million images from the ImageNet database that supports up to 19 layers. It can classify images into 1000 object categories such as many animals, pencils, pens, etc [32].

iii. Inception model

Inception Net is a victory over the previous versions of CNN models as previous models used to compromise the computation cost. Inception on the other hand reduces the computational cost to a great extent without compromising speed and accuracy [33]. Neural network architecture is constructed using the dimension-reduced inception module known as GoogLeNet (Inception v1). It is a widely used image recognition model. It is a CNN that is 22 layers deep (27, including the pooling layers). It uses a lot of tricks to push performance and is heavily engineered, both in terms of speed and accuracy.

For example, The models take an image of a car as the input and then predict the Make, Model and Year of the car. The models should be trained on the Cars Dataset. For transfer learning, the Inception-v3 architecture with pre-trained weights is to be used.

iv. Xception model

The Xception Model is proposed by Francois Chollet. It is an extension of the inception architecture which replaces the standard Inception modules with depth wise separable convolutions[34].

The Xception CNN was developed by Google Inc. as an ''extreme'' version of the Inception model. It is 71 layers deep. It outperforms inception on large scale image classification dataset because of modified depthwise separable convolution[35].

III. TRANSFER LEARNING WITH CONVOLUTIONAL NEURAL NETWORK:

Transfer learning refers to reusing the knowledge learned from one task for another. Specifically for CNNs, many image features are common to a variety of datasets. Hence, especially for large structures, CNNs are very rarely trained completely from scratch as large datasets and heavy computational resources are hard to come by.

In deep learning, transfer learning requires an initial training of a CNN for a given task, using large datasets. The availability of a sizable dataset is the main factor to ensure the success of the method since CNN can learn to extract the most significant features of a sample. CNN is considered suitable for transfer learning if it is found to be able to extract the most important image features.

Then, in transfer learning, CNN is used to analyse a new dataset of distinct nature and extract its features based on knowledge acquired in the first training. One strategy to exploit the capabilities of the pre-trained CNN is called feature extraction via transfer learning. By feature extraction, the CNN will retain its architecture and weights between its layers; therefore, CNN is used only as a feature extractor. The features are later used in a second network/classifier to process its classification.

In medical applications, the most accepted practice of transfer learning is to utilise the CNNs that achieved the best results in the ImageNet large scale visual recognition challenge (ILSVRC), which evaluates algorithms for object detection and classification on large scales. The use of large datasets for the initial training of CNN enables high performance in smaller datasets. This performance is linked to various extraction parameters that are typically not

 DOI : 10.35291/2454-9150.2021.0270

allowed as they can cause overfitting of the network. That said, feature extraction performed with transfer learning allows a large number of features to be extracted by generalising the problem and avoiding excessive adjustments.

The transfer learning method is applied in the feature extraction step for COVID-19 detection. The process is detailed in the below section.

IV. PROCEDURE

This section presents the proposed methodology for classifying an X-Ray and CT Scan of a healthy patient and patients suffering from COVID-19. First, we describe the datasets of images utilized in this study. Then, we explain the method of feature extraction, which is predicated on the transfer learning theory. After that, we present the classification techniques applied and therefore the steps of their training process. Lastly, we define the metrics we use to gauge the results and to match them to other approaches. Each step is explained in the next subsections.

A. Datasets

In this study, we used X-Ray and CT-Scan Multimodal Imaging Techniques to represent the frontal view of the chest. PA (posterior-anterior) view of the chest is used which examines the lungs, bony thoracic cavity, mediastinum and great vessels[36]. Thereafter, we divide the datasets into two parts: X-Ray images represented in this paper as Dataset A and CT-Scan images represented as Dataset B. Both of these datasets contain covid-19 patients and healthy patients images. In the first dataset i.e. Dataset A, the COVID-19 class is composed of 435 images of chest X-Ray of patients diagnosed with COVID-19, which were collected from different sources [37], [38]. They contain compilations of X-Ray images taken from different papers, databases, and other sources. For this dataset, we assembled the set of chest X-Ray images of healthy patients from the "Chest X-Ray Images (Pneumonia)" challenge on Kaggle[39]. We randomly selected 505 samples from the X-Ray images labelled them as "normal", which correspond to healthy patients. This source was chosen since it's been commonly utilized in related works that propose methods of detecting COVID-19 in X-Ray. Though, all the X-Ray images from this source are of pediatric patients.

In Dataset B, as previously mentioned, we grouped CT-Scan Images of the chest containing two classes 'normal' and 'covid-19'. For this dataset, we used images from the "NIH Chest X-rays" challenge organized by the National Institutes of Health on Kaggle[40]. We arbitrarily selected 397 images from the category of "no findings", which correspond to healthy patients. The covid-19 class consists of a total of 349 images. All images from the datasets are either within the joint photographic expert group (JPG/JPEG) or the portable network graphics (PNG) format. The image resolution within the dataset is 224 by 224 pixels.

Table I shows architectures used in the study along with their configurations and sizes to which the images were resized for each specific CNN.

Table I: CNN Architectures with their configurations and size of input images.

Architectures	Configurations	Input Image size (In Pixels)
ResNet	RESNET	224x224
Inception	InceptionV3	224x224
Xception	Xception	224x224
VGG	VGG16	224x224

Nevertheless, all images were pre-processed using the resizing technique. We present samples of images from the datasets in FIG 2. FIG 2.1(a) contains an X-Ray of Healthy Patients and FIG 2.1(b) Covid-19 patients. Similarly, Fig 2.2(a) consists of a CT-Scan of Healthy Patients and Fig 2.2(b) Covid-19 Patients respectively.

FIG 2

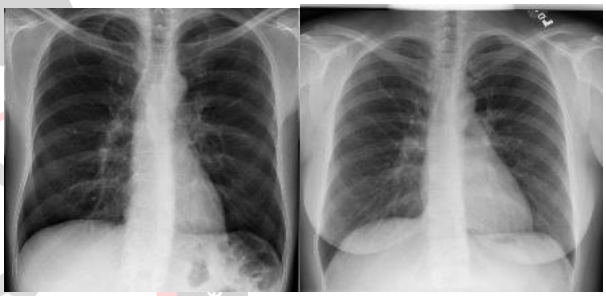

(a) **(b)**

FIG 2.1: X-Ray of Healthy Patient (a) vs X-ray of Covid-19 Positive Patient (b).

(a) **(b)**

FIG 2.2: CT-Scan of Healthy Patient (a) vs CT-Scan of Covid-19 Positive Patient (b).

The images were randomly selected to change. The transformations that were applied during this study were rotation, change in breadth, height, and magnification.[41]

B. Final Stage

We use the transfer learning concept discussed in section IV

 DOI : 10.35291/2454-9150.2021.0270

to initiate feature extraction from the X-Ray and CT-Scan images. First of all, we select different CNN architectures that achieved top performance on the ImageNet dataset. Then, we select different configurations, previously trained on ImageNet, from the chosen CNN architectures. After this, we remove any fully connected layers from these configurations, leaving only convolutional and pooling layers. These two sorts of layers are liable for extracting features from the image, while the fully connected ones are liable for classifying the features and, consequently, the image. Thus, removing these layers is important to show a CNN into a feature extractor. After this step, the new output from the adapted CNN is a set of features extracted from an input image. We built a sub-dataset for each of the CNN configurations composed of sets of features acquired from each image of the first datasets. To build a sub-dataset, we first resize each one of the images according to the size of inputs required by the selected CNN. Then, each resized image is employed as input to the CNN, and its set of features is extracted and stored within the corresponding sub-dataset. In Table I, we show all the CNN architectures and their respective configurations used. Table I also presents the input image size required by each configuration.

C. Classification Steps

We chose widely used machine learning methods in the literature to classify the X-Ray images and CT-Scan images: Bayes Classifier, which is the default classifier.

The classification is performed in three steps: First, model training. Second, model testing, and last, repetition of the first and second processes. Each sub-dataset is made of features extracted from the extractors presented in Section V-A. These sub-datasets are subdivided into 80% for training and the remaining for testing.

Table II: Number of X-Ray and CT-Scan images with Test and Train Dataset.

Dataset	A (X-Ray)		B(CT-Scan)	
	Train	Test	Train	Test
Covid-19 Images	331	83	280	69
Healthy Images	404	101	317	80
Total Images	919		746	

1. **Model Training:** In this step, we use 80% of the sub-dataset to train the model. We study the setup for the hyper-parameters to find the configuration of the classifiers on the training set. Each classifier has optimal hyperparameters, which are saved on the computer.
2. **Model Testing:** In this step, we perform a test in the remaining 20% of the sub-dataset using the trained classifiers. The system determines a one-one class for each sample of the sub-dataset. In addition to this, the metrics are calculated in this step.
3. **Repetition of Processes 1) and 2):** The sub-datasets are randomly split into other train and test sets. of data. These sets are assured to be different from the rest by the seed used. Then, we perform ten repetitions for steps 1) and 2).

D. Evaluation Metrics

We analyse the results of this paper utilising the metrics: accuracy (Acc), F1-score, and false-positive rate (FPR). Accuracy describes how often the model is classified correctly and accurately. F1-score can be described as the harmonic means of Precision and Sensitivity; this metric can provide a number that suggests an overall quality of the approach. FPR indicates the rate of healthy patients being wrongly classified. True Positives (TP) indicates the number of instances in which images are classified as COVID-19 by the model correctly. True Negatives (TN) inform the number of healthy patient images correctly classified by the model. False Positives (FP) points out the number of times that the model classified a healthy patient incorrectly. False Negative (FN) corresponds to the number of occasions that the COVID-19 images were misclassified as from a healthy patient. The equations for Sensitivity, Acc, FPR, Precision, and F1-score are presented on (1)–(5), respectively.

$$Acc(\%) = [(TP+TN)/(TP+FN+FP+TN)]\times 100 \quad \text{------- (1)}$$

$$Sensitivity = TP/(TP+FN) \quad \text{------- (2)}$$

$$Precision = TP/(TP+FP) \quad \text{------- (3)}$$

$$FPR(\%) = FP/(FP+TN)\times 100 \quad \text{------- (4)}$$

$$F1{-}score(\%)=2\times(Sensitivity\times Precision/Sensitivity+Precision\times 100. \quad \text{------- (5)}$$

In addition to the metrics already discussed, we also analyse the training, extraction, and test times. The training time symbolises the length of the period it takes from the beginning of the classifier training to the moment it gets ready to perform the classification process. Extraction time measures and calculates how long the adapted CNN takes to output the attribute vector from the moment it receives the X-Ray and CT-Scan. Also, the test time is the duration it takes for the classifier to predict and classify the image into a class after receiving its attribute vector. Thus, training time is vital during model building. After this step, the extraction and also the test times are more relevant and to the point. Their aggregate represents the classification time, which is the period between receiving the images and returning its class.

V. RESULTS

1. CT-Scan

For CT-Scan, the model was trained using InceptionV3, RESNET, VGG and Xception. We take the formulae as

 DOI : 10.35291/2454-9150.2021.0270

described in section V-D to calculate Accuracy, Sensitivity, Precision, F1-Score and FPR. The results of each model are as follows:

Table I: Values of Sensitivity, Precision, Accuracy, F1-Score and FPR% for CT-Scan images for respective models.

Model	Inception	RESNET	VGG	Xception
Sensitivity	0.62	0.12	0.69	0.6
Precision	0.86	0.73	0.92	0.75
Accuracy (%)	76	53.91	81.6	70.5
F1-score(%)	72.05	20.61	78.85	66.66
FPR(%)	10	4.2	5.7	19

(i) Inception: As we can see in Table I, the value of Sensitivity and Precision for this model is 0.62 and 0.86 respectively. In terms of percentage for this model, the Accuracy to detect the correct label of the image is 76%. F1-Score ‘s value is 72.05%. The wrongly classified images can be given by FPR whose value in percentage for this model is 10%.

FIG 3 gives a confusion matrix for the Inception model that helps us deduce the values of True Positive(TP)=0.62, True Negative(TN)=0.9, False Positive(FP)=0.1, False Negative(FN)=0.38.

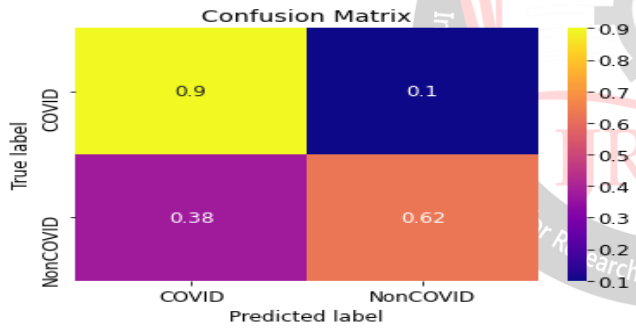

FIG 3 : Confusion Matrix of Inception model for CT-Scan images

(ii) RESNET: As we can see in Table I, the value of Sensitivity and Precision for this model is 0.12 and 0.73 respectively. The Accuracy in terms of percentage for this model to detect the correct label of the image is 53.91%, which is the lowest in comparison to other models. F1-Score ‘s value is 20.61%. The wrongly classified images can be given by FPR whose value in percentage for this model is 4.2%.

FIG 4 gives a confusion matrix of RESNET model that helps us deduce the values of True Positive(TP)=0.12, True Negative(TN) = 0.96, False Positive(FP)=0.043, False Negative(FN)=0.88.

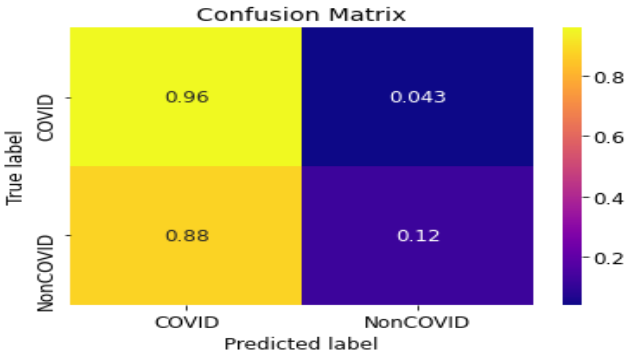

FIG 4: Confusion Matrix of RESNET model for CT-Scan images

(iii) VGG: As we can see in Table I, the value of Sensitivity and Precision for this model is 0.69 and 0.92 respectively. The Accuracy in terms of percentage for this model to detect the correct label of the image is 81.6%, which is highest in comparison to other models. F1-Score ‘s value is 78.85%. The wrongly classified images can be given by FPR whose value in percentage for this model is 5.7%.

FIG 5 gives a confusion matrix of VGG model that helps us deduce the values of True Positive(TP)=0.69, True Negative(TN)=0.94, False Positive(FP)=0.057, False Negative(FN)=0.31.

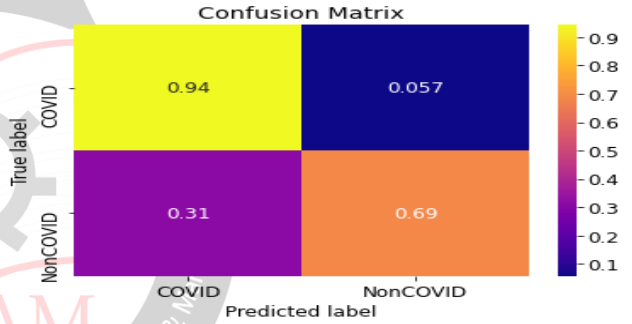

FIG 5: Confusion Matrix of VGG model for CT-Scan images

(iv) Xception: As we can see in Table I, the value of Sensitivity and Precision for this model is 0.6 and 0.75 respectively. In terms of percentage for this model, the Accuracy to detect the correct label of the image is 70.5%. F1-Score ‘s value is 66.66%. The wrongly classified images can be given by FPR whose value in percentage for this model is 19%.

FIG 6 gives a confusion matrix of the Xception model that helps us deduce the values of True Positive(TP)=0.6, True Negative(TN)=0.81, False Positive(FP)=0.19, False Negative(FN)=0.4.

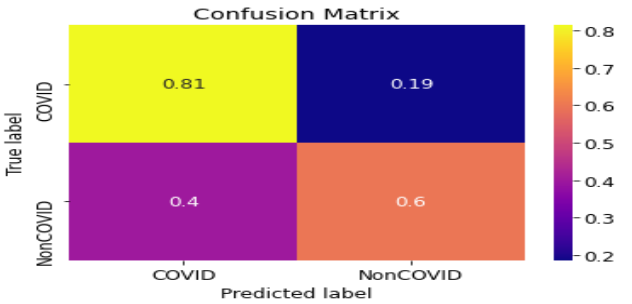

FIG 6: Confusion Matrix of Xception model for CT-Scan images

 DOI : 10.35291/2454-9150.2021.0270

2. X-Ray:

For X-Ray as well, the model was trained using InceptionV3, RESNET, VGG and Xception. We take the formulae as described in section V-D to calculate Accuracy, Sensitivity, Precision, F1-Score and FPR. The results of each model are as follows:

TABLE II: Values of Sensitivity, Precision, Accuracy, F1-Score and FPR% for X-Ray images for respective models.

Model	Inception	RESNET	VGG	Xception
Sensitivity	0.95	0.57	0.91	0.89
Precision	0.84	0.95	0.83	0.94
Accuracy (%)	89.00	61.37	87.54	85.18
F1-score(%)	89.16	71.25	86.20	91.43
FPR(%)	17	22.58	15.59	6.31

(i) Inception: As we can see in Table II, the value of Sensitivity and Precision for this model is 0.94 and 0.84 respectively. The Accuracy in terms of percentage for this model to detect the correct label of the image is 89%, which is the highest in comparison to other models. F1-Score 's value is 89.16%. The wrongly classified images can be given by FPR whose value in percentage for this model is 17%.

FIG 7 gives a confusion matrix of Inception model that helps us deduce the values of True Positive(TP)=0.95, True Negative(TN)=0.83, False Positive(FP)=0.17, False Negative(FN)=0.05.

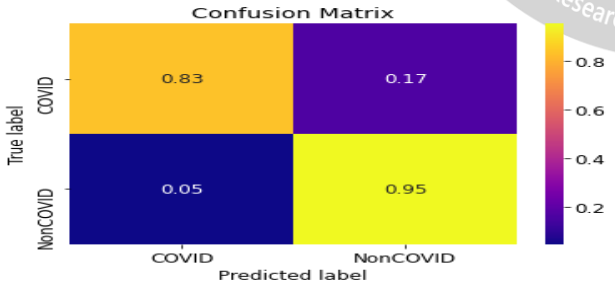

FIG 7: Confusion Matrix of Inception model for X-Ray images

(ii) RESNET: As we can see in Table II, the value of Sensitivity and Precision for this model is 0.57 and 0.95 respectively. The Accuracy in terms of percentage for this model to detect the correct label of the image is 61.37%, which is the lowest in comparison to other models. F1-Score 's value is 71.25%. The wrongly classified images can be given by FPR whose value in percentage for this model is 22.58%.

FIG 8 gives a confusion matrix of RESNET model that helps us deduce the values of True Positive(TP)=0.31, True Negative(TN)=0.92, False Positive(FP)=0.084, False Negative(FN)=0.69.

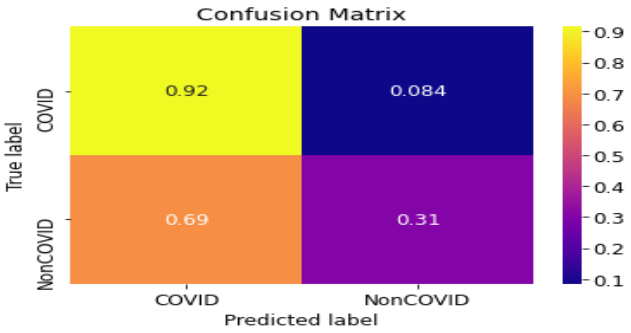

FIG 8: Confusion Matrix of RESNET model for X-Ray images

(iii) VGG: As we can see in Table II, the value of Sensitivity and Precision for this model is 0.91 and 0.83 respectively. In terms of percentage for this model, the Accuracy to detect the correct label of the image is 87.54%. F1-Score 's value is 86.20%. The wrongly classified images can be given by FPR whose value in percentage for this model is 15.59%.

FIG 9 gives a confusion matrix of VGG model that helps us deduce the values of True Positive(TP)=0.92, True Negative(TN)=0.83, False Positive(FP)=0.17, False Negative(FN)=0.079.

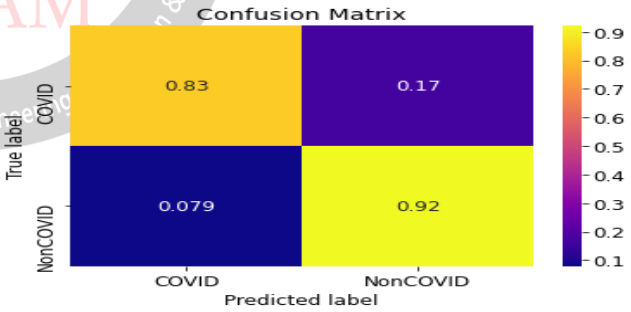

FIG 9: Confusion Matrix of VGG model for X-Ray images

(iv) Xception: As we can see in Table II, the value of Sensitivity and Precision for this model is 0.89 and 0.94 respectively. In terms of percentage for this model, the Accuracy to detect the correct label of the image is 85.18%. F1-Score 's value is 91.43%. The wrongly classified images can be given by FPR whose value in percentage for this model is 6.31%.

FIG 10 gives a confusion matrix of Xception model that helps us deduce the values of True Positive(TP)=0.89, True Negative(TN)=0.94, False Positive(FP)=0.06, False Negative(FN)=0.11.

 DOI : 10.35291/2454-9150.2021.0270

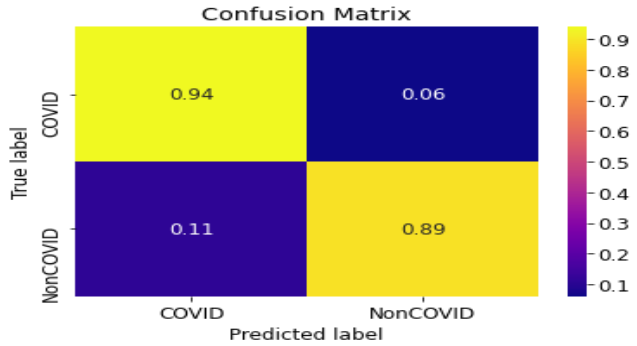

FIG 10: Confusion Matrix of Xception model for X-Ray images

VI. CONCLUSION

In this paper, we did a comparative study of the proof-of-concept hypothesis that COVID-19 contaminated patients can be diagnosed using X-Ray and CT Scan images. We pre-processed the CT Scan and X-Ray images by scaling them to 224 by 224 pixels, colour grading and altering the orientation. Doing this process allowed us to enhance the learning of the algorithms. Using transfer learning on pre-trained models, we were able to achieve high accuracy and save the training time of the models. The four pre-trained models on which we did the comparative study were namely, Inception, RESNET, VGG, and Xception.. These models were trained on our pre-processed dataset which contained the CT Scan and X-Ray images of both, COVID positive and COVID negative people.

Due to several mutated COVID variations with different symptoms, the procedure becomes more complicated thereby increasing the false-positive and false-negative parameters. Our model is reliable since it works with a considerable compact dataset, takes less time in detection and is cost-effective. In comparison to existing deep learning algorithms, the suggested transfer learning technique offers greater accuracy and takes much less time to train.

Upon testing the CT-Scan models, we can observe that all combinations in the top five achieved a reaching minimum accuracy of 70.5% and a minimum F1 score of 20.61%. However, the combination that should be highlighted is VGG, since it reached a maximum accuracy of 81.6%, a maximum F1-score of 78.85%, and a False-Positive rate of 5.7%.

With the X-Ray models, we can observe that all combinations in the top five achieved a reaching minimum accuracy of 61.37% and a minimum F1 score of 14.39%. However, the combination that should be highlighted is Inception, since it achieved an accuracy of 87.54% and an F1-score of 86.20%, and a False-Positive rate of 15.59%.

In a nutshell, by comparing accuracies of both multimodal imaging techniques i.e. X-Ray and CT-Scan, we conclude that X-Ray with Inception models is more accurate since it reaches the maximum accuracy of 89% while CT-Scan reaches the highest accuracy of 81.6% with the VGG model.

REFERENCES

[1] W. H. Organization, ``Coronavirus disease 2019 (COVID-19)," Situation Report 72, W. H. Organization, Geneva, Switzerland, 2020.

[2] COVID-19 History [Online] Available: https://www.webmd.com/lung/coronavirus-history.

[3] WHO COVID-19 Situation Reports. [Online]. Available:

www.who.int/emergencies/diseases/novel-coronavirus-2019

[4] C. Eastin and \T. Eastin, ``Clinical characteristics of coronavirus disease 2019 in China," J. Emergency Med., vol. 58, no. 4, pp. 711_712, Apr. 2020.

[5]Y. H. Xu, J. H. Dong, W. M. An, X. Y. Lv, X. P. Yin, J. Z. Zhang, L. Dong, X. Ma, H. J. Zhang, and B. L. Gao, "Clinical and computed tomographic imaging features of novel coronavirus pneumonia caused by sars-cov-2," J. Infect., vol. 80, no. 4, pp. 394–400, Apr. 2020.

[6] D. M. Musher and A. R. Thorner, ``Community-acquired pneumonia," New England J. Med., vol. 371, no. 17, pp. 1619_1628, 2014.

[7] K. Tolksdorf, S. Buda, E. Schuler, L. H. Wieler, and W. Haas, ``In_uenzaassociated pneumonia as a reference to assess the seriousness of coronavirus disease (COVID-19)," Eurosurveillance, vol. 25, no. 11, Mar. 2020, Art. no. 2000258.

[8] G. Grasselli, A. Pesenti, and M. Cecconi, ``Critical care utilization for the COVID-19 outbreak in Lombardy, Italy: Early experience and forecast during an emergency response," JAMA, vol. 323, no. 16, p. 1545, Apr. 2020.

[9] W.Wang, Y. Xu, R. Gao, R. Lu, K. Han, G.Wu, andW. Tan, ``Detection of SARS-CoV-2 in different types of clinical specimens," JAMA, vol. 323, pp. 1843_1844, Mar. 2020, DOI: 10.1001/jama.2020.3786.

[10] C. Chen, G. Gao, Y. Xu, L. Pu, Q. Wang, L. Wang, W. Wang, Y. Song, M. Chen, L. Wang, F. Yu, S. Yang, Y. Tang, L. Zhao, H. Wang, Y. Wang, H. Zeng, and F. Zhang, ``SARS-CoV-2_positive sputum and faeces after conversion of pharyngeal samples in patients with COVID-19," Ann. Internal Med., vol. 172, no. 12, pp. 832_834, Jun. 2020, DOI: 10.7326/M20-0991.

[11] T. Ai, Z. Yang, H. Hou, C. Zhan, C. Chen, W. Lv, Q. Tao, Z. Sun, and L. Xia, ``Correlation of chest CT and RT-PCR testing for coronavirus disease 2019 (COVID-19) in China: A report of 1014 cases," Radiology, vol. 296, no. 2, pp. E32_E40, Aug. 2020, doi:10.1148/radiol.2020200642.

[12] M. Hosseiny, S. Kooraki, A. Gholamrezanezhad, S. Reddy, and L. Myers, ``Radiology perspective of coronavirus disease 2019 (COVID-

[13] A. Ulhaq, A. Khan, D. Gomes, and M. Paul, ``Computer vision for COVID-19 control: A survey," 2020, arXiv:2004.09420. [Online]. Available:

http://arxiv.org/abs/2004.09420

[14] J. Born, G. Brändle, M. Cossio, M. Disdier, J. Goulet, J. Roulin, and N. Wiedemann, ``POCOVID-net: Automatic detection of COVID-19 from a new lung ultrasound imaging dataset (POCUS)," 2020,

arXiv:2004.12084. [Online]. Available: http://arxiv.org/abs/2004.12084

[15]Y. Li and L. M. Xia, "Coronavirus disease 2019 (COVID-19): Role of chest CT in diagnosis and management," Am. J. Roentgenol., vol. 214, no. 6, pp. 1280–1286, Jun. 2020.

 DOI : 10.35291/2454-9150.2021.0270

[16] Can X-ray chest decide the severity of COVID infection by Dr KK Aggarwal, President of Heart Care Foundation of India Available: https://www.youtube.com/watch?v=-jgTN1V0e74

[17] (2020). *ACR Recommendations*. [Online]. Available: https://www.acr.org/Advocacy-and-Economics/ACR-Position-Statements/Recommendations-for -Chest-Radiography-and-CT-for-Suspected-COVID19-Infection

[18] R. Yamashita, M. Nishio, R. K. G. Do, and K. Togashi, ``Convolutional neural networks: An overview and application in radiology," *Insights into Imag.*, vol. 9, no. 4, pp. 611_629, Aug. 2018, DOI: 10.1007/s13244-018-0639-9.

[19] M. A. Mazurowski, M. Buda, A. Saha, and M. R. Bashir, ``Deep learning in radiology: An overview of the concepts and a survey of the state of the art with a focus on MRI," *J. Magn. Reson. Imag.*, vol. 49, no. 4, pp. 939_954, Apr. 2019, DOI: 10.1002/jmri.26534.

[20] H. Ravishankar, P. Sudhakar, R. Venkataramani, S. Thiruvenkadam, P. Annangi, N. Babu, and V. Vaidya, ``Understanding the mechanisms of deep transfer learning for medical images," in *Deep Learning and* *Data Labeling for Medical Applications* (Lecture Notes in Computer Science), vol. 10008, G. Carneiro, Ed. Cham, Switzerland: Springer, 2016, pp. 188_196, DOI: 10.1007/978-3-319-46976-820.

[21] Y. Yu, H. Lin, J. Meng, X. Wei, H. Guo, and Z. Zhao, ``Deep transfer learning for modality classi_cation of medical images," *Information*, vol. 8, no. 3, p. 91, Jul. 2017, DOI: 10.3390/info8030091.

[22] S. J. Pan and Q. Yang, "A survey on transfer learning," *IEEE Trans. Knowl. Data Eng.*, vol. 22, no. 10, pp. 1345–1359, Oct. 2009.

[23] K. Weiss, T. M. Khoshgoftaar, and D. D. Wang, "A survey of transfer learning," *J. Big data*, vol. 3, no. 1, pp. 9, Oct. 2016.

[24] M. Huh, P. Agrawal, and A. A. Efros, "What makes imagenet good for transfer learning?" arXiv preprint arXiv: 1608.08614, 2016.

[25] The procedure of Transfer Learning in Feature Extraction [Online]. Available: https://www.researchgate.net/figure/The-figure-shows-the-procedure-of-transfer-learning-in-feature-extraction-of-VGG-19_fig3_335358213

[26] Residual Network (ResNet)[Online]. Available:https://iq.opengenus.org/resnet/

[27] Understanding and implementation of Residual Networks(ResNets)[Online]. Available: https://medium.com/analytics-vidhya/understanding-and-implementation-of-residual-networks-resnets-b80f9a507b9c

[28] Residual blocks — Building blocks of ResNet[Online]. Available: https://towardsdatascience.com/residual-blocks-building-blocks-of-resnet-fd90ca15d6ec

[29] VGG Neural Networks: The Next Step After AlexNet[Online]. Available: https://towardsdatascience.com/vgg-neural-networks-the-next-step-after-alexnet-3f91fa9ffe2c

[30] What is the difference between VGG16 and VGG19 neural networks? [Online]. Available: https://www.quora.com/What-is-the-difference-between-VGG16-and-VGG19-neural-network

[31] VGG16 – Convolutional Network for Classification and Detection [Online]. Available: https://neurohive.io/en/popular-networks/vgg16

[32] MathWorks-VGG19 [Online]. Available: https://www.mathworks.com/help/deeplearning/ref/vgg19.html;jsessionid=94509bad224d49e0405d217e2d99

[33] ML | Inception Network V1[Online]. Available: https://www.geeksforgeeks.org/ml-inception-network-v1

[34] ImageNet: VGGNet, ResNet, Inception, and Xception with Keras[Online]. Available: https://www.pyimagesearch.com/2017/03/20/imagenet-vggnet-resnet-inception-xception-keras/

[35] Review: Xception — With Depthwise Separable Convolution, Better Than Inception-v3 (Image Classification)[Online]. Available: https://towardsdatascience.com/review-xception-with-depthwise-separable-convolution-better-than-inception-v3-image-dc967dd42568

[36] Chest (PA view)- Radiopaedia [Online]. Available: https://radiopaedia.org/articles/chest-pa-view-1

[37] J. P. Cohen, P. Morrison, and L. Dao, "Covid-19 image data collection," arXiv preprint arXiv: 2003.11597, 2020.

[38] COVID-19 X rays. [Online]. Available: https://www.kaggle.com/andrewmvd/convid19-x-rays

[39] D. S. Kermany, M. Goldbaum, W. J. Cai, C. C. S. Valentim, H. Y. Liang, S. L. Baxter, A. McKeown, G. Yang, X. K. Wu, F. B. Yan, J. Dong, M. K. Prasadha, J. Pei, M. Y. L. Ting, J. Zhu, C. Li, S. Hewett, J. Dong, I. Ziyar, A. Shi, R. Z. Zhang, L. H Zheng, R. Hou, W. Shi, X. Fu, Y. O. Duan, V. A. N. Huu, C. Wen, E. D. Zhang, C. L. Zhang, O. L. Li,

X. B. Wang, M. A. Singer, X. D. Sun, J. Xu, A. Tafreshi, M. A. Lewis, H. M. Xia, and K. Zhang, "Identifying medical diagnoses and treatable diseases by image-based deep learning," Cell, vol.172, no. 5, pp.1122–1131.E9, Feb. 1122.

[40] X. S. Wang, Y. F. Peng, L. Lu, Z. Y. Lu, M. Bagheri, and R. M. Summers, "Chestx-ray8: Hospital-scale chest X-ray database and benchmarks on weakly supervised classification and localization of common thorax diseases, " in Proc. IEEE Conf. Computer Vision and Pattern Recognition, Honolulu, HI, USA, 2017, pp. 3462–3471.

[41] A. Mikołajczyk and M. Grochowski, "Data augmentation for improving deep learning in an image classification problem, " in Proc. Int. Interdisciplinary PhD Workshop, Swinoujście, Poland, 2018, pp. 117–122.

 DOI : 10.35291/2454-9150.2021.0270